The W105G and W99G Sorcin Mutants Demonstrate the Role of the D Helix in the Ca^{2+}-Dependent Interaction with Annexin VII and the Cardiac Ryanodine Receptor†

Gianni Colotti,‡ Carlotta Zamparelli,‡ Daniela Verzili,‡ Manuela Mella,‡ Christopher M. Loughrey,§,|| Godfrey L. Smith,§ and Emilia Chiancone*,‡

Consiglio Nazionale delle Ricerche Institute of Molecular Biology and Pathology, Department of Biochemical Sciences A. Rossi Fanelli, University of Rome La Sapienza, 00185 Rome, Italy, and Institute of Biomedical and Life Sciences, University of Glasgow, Glasgow G12 8QQ, United Kingdom

Received March 2, 2006; Revised Manuscript Received August 22, 2006

ABSTRACT: Sorcin, a 21.6 kDa two-domain penta-EF-hand (PEF) protein, when activated by Ca^{2+} binding, interacts with target proteins in a largely uncharacterized process. The two physiological EF-hands EF3 and EF2 do not belong to a structural pair but are connected by the D helix. To establish whether this helix is instrumental in sorcin activation, two D helix residues were mutated: W105, located near EF3 and involved in a network of interactions, and W99, located near EF2 and facing solvent, were substituted with glycine. Neither mutation alters calcium affinity. The interaction of the W105G and W99G mutants with annexin VII and the cardiac ryanodine receptor (RyR2), requiring the sorcin N-terminal and C-terminal domain, respectively, was studied. Surface plasmon resonance experiments show that binding of annexin VII to W99G occurs at the same Ca^{2+} concentration as that of the wild type, whereas W105G requires a significantly higher Ca^{2+} concentration. Ca^{2+} spark activity of isolated heart cells monitors the sorcin−RyR2 interaction and is unaltered by W105G but is reduced equally by W99G and the wild type. Thus, substitution of W105, via disruption of the network of D helix interactions, affects the capacity of sorcin to recognize and interact with either target at physiological Ca^{2+} concentrations, while mutation of solvent-facing W99 has little effect. The D helix appears to amplify the localized structural changes that occur at EF3 upon Ca^{2+} binding and thereby trigger a structural rearrangement that enables interaction of sorcin with its molecular targets. The same activation process may apply to other PEF proteins in view of the D helix conservation.

Sorcin (SOluble Resistance-related Calcium binding proteIN) belongs to the penta-EF-hand (PEF)[1] family, a small group of Ca^{2+}-binding proteins that comprises calpains (*1*, *2*), grancalcin (*3*), ALG-2 (*4*), and peflin (*5*). The binding of Ca^{2+} triggers the reversible translocation of all PEF proteins from the cytoplasm to cell membranes where they interact with specific target proteins and thereby participate in a variety of physiological processes. The molecular mechanism of the Ca^{2+}-linked activation process is largely unknown, although a major role has been assigned to the long and rigid D helix located in the C-terminal domain, a compact, highly conserved structure that contains the five EF-hands (*6*). The D helix is unusual in that it is shared by two EF-hands belonging to different structural pairs, namely, by EF2 and EF3, a peculiarity that pertains also to the G helix which is shared by EF4 and EF5. The latter helix has a clear structural role as it gives rise to a stable interface between two monomers together with the H helix. Upon dimer formation, the two odd EF5 motifs interact with each other and achieve the canonical structural pairing of EF-hands (*7*−*10*). In contrast to the C-terminal domain, the N-terminal domain is of variable length across the range of PEF proteins but is always rich in glycine and proline residues. Because of the flexibility that this endows, the N-terminus is not visible in most available X-ray crystal structures (*8*, *9*).

The conformational change that permits interaction of PEF proteins with targets entails exposure of hydrophobic residues and is triggered by the binding of two Ca^{2+} ions per monomer. In a recent study with site-specific sorcin variants carrying mutations at the Ca^{2+} binding loops, EF3 and EF2 have been identified as the two functional EF-hands since Ca^{2+} affinity decreases in the following order: EF3 > EF2 > EF1. Moreover, since the D helix connects the structurally distant EF3 and EF2 hands and contains an extended hydrophobic patch, it was hypothesized to be instrumental in Ca^{2+}-induced activation of sorcin (*6*). A molecular description of these processes requires an understanding of the mechanism underlying the transfer of information about

† This study was funded by the British Heart Foundation (to G.L.S.) and by the Ministero Istruzione Università e Ricerca, PRIN 2005 (to E.C.).

* To whom correspondence should be addressed: Department of Biochemical Sciences A. Rossi Fanelli, University of Rome La Sapienza, 00185 Rome, Italy. Telephone: +390649910761. Fax: +39064440062. E-mail: emilia.chiancone@uniroma1.it.

‡ Consiglio Nazionale delle Richerche−IBPM, University of Rome La Sapienza.

§ University of Glasgow.

|| Current address: Institute of Comparative Medicine, University of Glasgow, Glasgow G12 8QQ, United Kingdom.

[1] Abbreviations: PEF, penta-EF-hand; PVDF, polyvinyl difluoride; RyR1, skeletal muscle ryanodine receptor; RyR2, cardiac ryanodine receptor; SCBD, sorcin Ca^{2+}-binding domain; SPR, surface plasmon resonance; SR, sarcoplasmic reticulum.

10.1021/bi060416a CCC: $33.50
Published on Web 09/26/2006

A

N-terminal domain

MAYPGHPGAGGGYY**PGGYGGAPGGP**SFPGQTQ 1-32

C-terminal domain (SCBD)

Helix A *EF1* *Helix B* *Helix C* *EF2*
DPLYGYFASVAGQDGQIDADELQRCLTQSGIAGGYKPFNLETCRLMVSMLDRDMSGTMG 33-91

Helix D *EF3* *Helix E* *Helix F*
FNEFKEL**W**AVLNG**W**RQHFISFDSDRSGTVDPQELQKALTTMGFRLNPQTVNSIAKR 92-147

EF4 *Helix G* *EF5* *Helix H*
YSTSGKITFDDYIACCVKLRALTDSFRRRDSAQQGMVNFSYDDFIQCVMTV 148-198

B

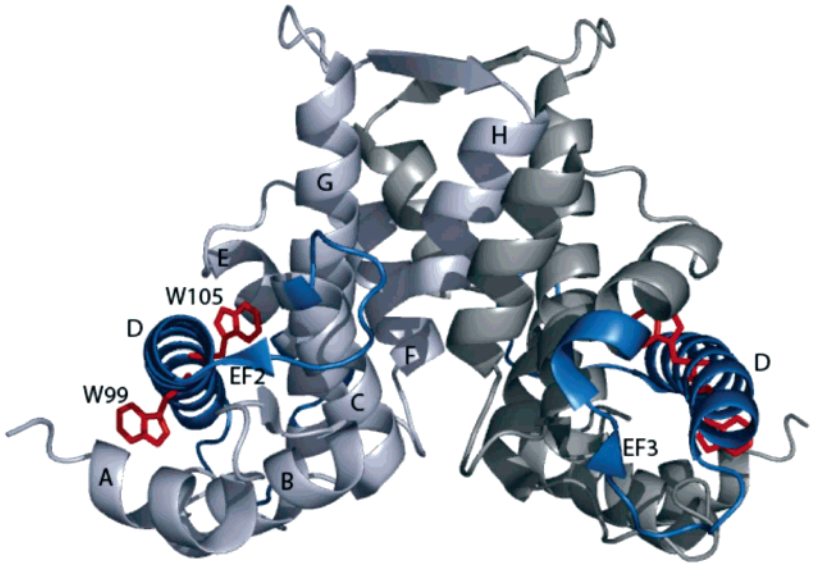

FIGURE 1: Sorcin sequence (A) and structure of the Ca^{2+}-binding domain, SCBD (B). In panel A, the 11 amino acids which interact with SCBD in the model of Ilari et al. (*7*) are in boldface. In panel B, the two monomers are depicted in different colors. The D helix and physiologically relevant EF2 and EF3 are colored blue; the two tryptophan residues, W99 and W105, are colored red. This figure was created with PYMOL (*36*).

the Ca^{2+} binding event from EF3 to the rest of the molecule and the nature of the ensuing structural rearrangements. Surprisingly, the reported Ca^{2+}-dependent changes in the crystal structures of known PEF proteins are rather subtle and are localized to the EF1−EF2 pair, close to the connection between the N- and C-terminal domains (*1*, *9*, *11*−*13*). It is not known how such small changes are amplified to the extent required for target protein interaction. In the case of sorcin, Ilari et al. (*7*) proposed an activation mechanism based on the X-ray crystal structure of the C-terminal domain (SCBD, sorcin Ca^{2+}-binding domain, corresponding to residues 33−198) that accounts for the increased hydrophobicity of the Ca^{2+}-bound protein. Ca^{2+} binding is believed to cause a series of structural rearrangements that loosens the interactions between the N- and C-terminal domains, making them available for binding the respective targets.

This work was undertaken to validate this mechanism. Experiments were designed that take advantage of the presence of the only two tryptophan residues, W99 and W105, in the D helix. As shown in Figure 1, W99 is close to the EF2 Ca^{2+}-binding loop (~4 Å), whereas W105 is close to EF3 (~7 Å). The two tryptophan residues are one and one-half helical turns apart such that the side chain of W99 lies on the outer surface of the SCBD, in contact with residues that join the two domains, whereas the W105 side chain points toward the core of the SCBD where it interacts primarily with residues of the D and G helices (*7*). The different localization of the two tryptophan residues within the D helix and the different type of interactions they establish suggest that their substitution may affect differently the functional coupling of EF3 and EF2 and the interaction with target proteins. The involvement of W105 in the network of hydrophobic and hydrogen bonding interactions is expected to render this residue of major importance for the transmission of the Ca^{2+}-dependent conformational changes. To verify this contention, site-specific mutants W99G and W105G were produced and their interaction with annexin VII and with the cardiac ryanodine receptor (RyR2) (*14*), the main Ca^{2+} channel of cardiac sarcoplasmic reticulum (SR), was studied. Previous work has shown that annexin VII and the skeletal muscle ryanodine receptor (RyR1) interact with the sorcin N-terminal and C-terminal domain, respectively (*15*, *16*); RyR2 can be taken to behave like RyR1 given their structural similarity. In the case of RyR2, the possible influence of the N-terminal domain was assessed by comparing the isolated SCBD to the wild-type protein. Additionally, EF3 site variant E124A was employed as a control since it is unable to bind Ca^{2+} at physiological

concentrations due to substitution of Glu124 in position $-Z$ (*6*).

The sorcin−annexin VII interaction was studied directly by Western blot and surface plasmon resonance experiments, whereas the interaction of sorcin with RyR2 was monitored by measuring Ca^{2+} spark activity in isolated rabbit heart cells (*17*). Previous work has shown that addition of sorcin affects Ca^{2+} sparks in permeabilized myocytes (*18*, *19*). Although Ca^{2+} affinity is substantially unaltered in the two mutants with respect to the wild-type protein, substitution of W105 affects its capacity to recognize and interact with the two targets significantly, while mutation of W99 has an only small effect on sorcin function. These results support the crucial role of the D helix in sorcin activation (*6*, *7*) and in particular show that W105 is a major player in this process. Other PEF proteins are likely to use the same activation mechanism in view of the high degree of sequence conservation in the D helix (*20*).

MATERIALS AND METHODS

Cloning of the W99G and W105G Sorcin Variants. The cDNA of Chinese hamster ovary sorcin, cloned between the unique NdeI and HindIII sites of plasmid pET22 (Novagen) (*6*), was subjected to site-directed mutagenesis by the PCR overlap extension mutagenesis method, according to the method of Higuchi et al. (*21*).

The following oligonucleotides were used: Nforward, 5′-GCGAAATTAATACGACTCACTATAGGG-3′; Creverse, 5′-CAAGCTTTTAGACGGTCATGACAC-3′; W99G forward. 5′-GAATTTAAAGAGCTCGGCGCTGTGCTGAATGG-3′; W99G reverse. 5′-CCATTCAGCACAGCGCCGAGCTCTTTAAATTC-3′; W105G forward, 5′-CTGTGCTGAATGGCGGCAGACAACACTTCATC-3′; and W105G reverse, 5′-GATGAAGTGTTGTCTGCCGCCATTCAGCACAG-3′.

The PCR products that were obtained were agarose-purified, digested with NdeI and HindIII, and cloned into a pET22 expression vector (Novagen).

Expression and Purification of Wild-Type (wt) Sorcin and Its Variants. Chinese hamster ovary recombinant sorcin was expressed in *Escherichia coli* BL21(DE3) cells and purified as previously described (*22*). The same purification procedure was used for the site-specific mutants. Protein concentrations were determined spectrophotometrically at 280 nm. The molar extinction coefficients were calculated according to the method of Edelhoch (*23*) and were 29 400 for the wt protein, 22 640 for W99G, 22 640 for W105G, and 22 000 for SCBD.

Circular Dichroism and Fluorescence Spectra. CD spectra were recorded on a Jasco J-710 spectropolarimeter in the far-UV (200−250 nm) and near-UV (250−350 nm) regions. The experiments were carried out at 20 °C in 100 mM Tris-HCl at pH 7.5. The α-helical content was calculated from the ellipticity value at 222 nm (*24*) and with Selcon3 (srs.dl.ac.uk/VUV/CD/selcon.html).

Intrinsic fluorescence was measured in a Fluoromax spectrofluorimeter at 25 °C in 100 mM Tris-HCl at pH 7.5 using an excitation wavelength of 280 nm and a slit width of 0.5 nm. The emission signal was followed between 300 and 400 nm.

Analytical Ultracentrifugation. Sedimentation velocity experiments were carried out on a Beckman-Coulter ProteomeLab XL-I analytical ultracentrifuge at 40 000 rpm and 15 °C at a protein concentration of 1 mg/mL in 0.1 M Tris-HCl buffer at pH 7.5. The protein concentration gradient in the cells was determined by absorption scans along the centrifugation radius at 280 nm with three averages and a step resolution of 0.005 cm. Data were analyzed with SEDPHAT (sedimentation and polymer hydrodynamic analysis tool, www.analyticalultracentrifugation.com/sedphat/configurations.htm) and are expressed in terms of the weight-average molecular mass (M_w) by assuming a spherical shape of the molecule.

Determination of Ca^{2+} Affinity. Titrations based on the competitive chelator method (*25*) were carried out in 100 mM Tris-HCl at pH 7.5 and 25 °C using the fluorescent Ca^{2+} chelators Quin 2, as described in Zamparelli et al. (*26*), and Fluo-3. The excitation wavelength was 339 nm in the case of Quin 2 and 488 nm in the case of Fluo-3; the increment of emission intensity due to Ca^{2+} binding was followed for Quin 2 at 492 nm (slit width of 0.5 nm) and for Fluo-3 at 528 nm (slit width of 1 nm). The protein concentration in the experiments involving Quin 2 was 25 μM and in those with Fluo-3 was 15 μM.

Control experiments were performed on Quin 2 and on Fluo-3 alone. Special care was taken to reduce Ca^{2+} contamination to 0.5−1.0 μM by treating the protein solutions and the glassware with Chelex 100 as recommended by André and Linse (*27*). At the end of each titration, the fluorescence intensity corresponding to the nominally zero free Ca^{2+} concentration was determined by addition of 5 mM EGTA. The fluorescence intensity of Quin 2 or Fluo-3 at high Ca^{2+} concentrations was taken as the higher asymptote. The binding constants were assessed by fitting the experimental data with CaLigator (*27*) by using the [2 Ca^{2+} sites + chelator] model.

Overlay Assay Experiments. W99G and W105G were subjected to electrophoresis on a 15% polyacrylamide gel under denaturing conditions (*28*) and transferred to polyvinyl difluoride membranes (PVDF) in transfer buffer [25 mM Tris-HCl, 192 mM glycine, and 20% methanol (pH 8.3)] at 100 mA for 45 min. The PVDF membranes were incubated at room temperature with annexin VII (5 μg/mL) in 1% gelatin in TBST buffer [20 mM Tris-HCl, 0.5 M NaCl, and 0.05% Tween 20 (pH 7.5)] containing 1 mM EGTA or 10 or 75 μM $CaCl_2$ (total). Subsequently, the membranes were incubated with an anti-annexin VII monoclonal antibody kindly provided by A. Noegel (1:3000 dilution) in 1% gelatin in TBST buffer. The blots were developed by incubation for 2−5 min with alkaline phosphatase-conjugated monoclonal anti-mouse IgG in 1% gelatin in TBST. The longer incubation time was used for the blots carried out at <10 nM calcium (i.e., in 1 mM EGTA) to exclude any interaction; under these conditions, the ovalbumin molecular mass marker band shows positive staining. Control experiments ruled out the existence of cross reactivity between the sorcin variants and the anti-annexin VII monoclonal antibody.

Surface Plasmon Resonance Measurements. Surface plasmon resonance (SPR) experiments were carried out using a BIACORE X system (BIAcore AB, Uppsala, Sweden). The N-terminal peptide of annexin VII was synthesized by SIGMA-Genosys (Cambridge, U.K.); to improve peptide

solubility and binding to the sensor chip, three lysine residues were added to the N-terminal end of the 20 first amino acids of annexin VII (MSYPGYPPTGYPPFPGYPPA). The peptide purity was checked by MALDI-TOF mass spectrometry. The calculated isoelectric point of the peptide is 9.90, determined using pI-tool (*29*).

The sensor chip (CM5, Biacore AB) was activated chemically by injection of 35 μL of a 1:1 mixture of *N*-ethyl *N*′-[3-(dimethylamino)propyl]carbodiimide (200 mM) and *N*-hydroxysuccinimide (50 mM) at a flow rate of 5 μL/min. The N-terminal peptide of annexin VII was immobilized on the activated sensor chip via amine coupling. The reaction was carried out in 20 mM sodium acetate at pH 6.0; the remaining ester groups were blocked by injecting 1 M ethanolamine hydrochloride (35 μL). In control experiments, the sensor chip was treated as described above in the absence of peptide.

The interaction of the immobilized annexin VII peptide with wild-type sorcin, SCBD, and the variants was detected through mass concentration-dependent changes in the refractive index on the sensor chip surface. The changes in the observed SPR signal are expressed as resonance units (RU). A response change of 1000 RU typically corresponds to a change in the protein concentration on the sensor chip of ~1 ng/mm^2 (*30*).

The experiments were carried out at 25 °C in 10 mM HEPES (pH 7.4), 150 mM NaCl, and 0.005% surfactant P-20. The buffer was treated with Chelex 100 to eliminate Ca^{2+} contaminations and degassed. For the experiments as a function of Ca^{2+} concentration, calcium chloride or EGTA was added to the buffer; the protein concentration was 300 nM. Measurements were performed at a flow rate of 20 μL/min with an immobilization level of the annexin VII N-terminal peptide corresponding to 100−900 RU. All measurements were repeated twice using different sensor chips. The amine coupling kit, the P-20 surfactant, and the CM-5 sensor chip were purchased from BIAcore AB, and all the other reagents were high-purity grade.

Scatchard analysis of the dependence of the SPR signal at steady state (R_{eq}) on the concentration of sorcin was performed to assess the dissociation constant. R_{eq} values were calculated from the sensorgrams using BIAevaluation version 3.0.

Measurement of Ca^{2+} Spark Characteristics in Isolated Heart Cells. An investigation of the direct effects of sorcin on Ca^{2+} sparks in intact rabbit cardiomyocytes is complicated by the parallel effects on the sarcolemmal extrusion of intracellular Ca^{2+} (*19*). For this reason, sarcolemmal fluxes are bypassed by the acute permeabilization of the sarcolemma with β-escin. Under such experimental conditions, single cardiomyocytes can be superfused using the standardized Ca^{2+} concentration and pH in the presence of ATP and creatine phosphate. Ca^{2+} spark activity is monitored by the inclusion of 10 μM Fluo-3 in the perfusing solution. In this study, isolated rabbit ventricular cardiomyocytes were initially suspended in a mock intracellular solution with the following composition: 100 mM KCl, 5 mM Na_2ATP, 10 mM Na_2CrP, 5.5 mM $MgCl_2$, 25 mM HEPES, and 1 mM K_2EGTA (pH 7.0) with no added Ca^{2+} (20−21 °C). They were then permeabilized using β-escin (0.1 mg/mL for 0.5−1 min). Confocal line-scan images of single cardiomyocytes were recorded using a BioRad Radiance 2000 confocal system. Permeabilized cells were perfused with a mock intracellular solution containing 0.05 mM EGTA. Fluo-3 (10 μM) in the perfusing solution was excited at 488 nm (Kr laser line) and measured above 515 nm using epifluorescence optics of a Nikon Eclipse inverted microscope with a 60× 1.2 NA water-immersion objective lens (Plan Apochromat, Nikon). In all experiments included in the analysis, the Ca^{2+} concentration in the test solution was 155−165 nM. Ca^{2+} sparks were quantified using an automatic detection and measurement algorithm (*19*).

RESULTS

Characterization of the W99G and W105G Variants. Binding of two Ca^{2+} ions per sorcin monomer leads to the exposure of hydrophobic surfaces that manifests itself in the tendency of the wt protein to aggregate or precipitate in the absence of protein targets. This tendency, which limits the experimental conditions that can be used for the measurement of the Ca^{2+}-bound protein spectra (*26*), is particularly marked in the W105G variant.

The attempts made so far to obtain X-ray quality crystals of the two tryptophan variants have failed. Therefore, possible structural changes relative to the wt protein were monitored by means of CD and fluorescence spectroscopy and by analytical ultracentrifugation. The folding of the mutated apoproteins is essentially unaltered with respect to that of wild-type sorcin as indicated by the similarity of the far-UV CD spectra (Figure 2A). Analysis of the spectra points to a similar α-helix content, i.e., 60% for wt sorcin and 58% for both W99G and W105G. Support for the similarity of tertiary−quaternary structure was gained from the similarity of the weight-average molecular mass values (M_w) calculated from sedimentation velocity experiments (35 000 Da for wild-type sorcin, 36 500 Da for W99G, and 34 700 Da for W105G).

The occurrence of structural perturbations that are localized to the environment of the tryptophan residues and of other aromatic side chains is indicated by the near-UV CD and fluorescence emission spectra of the mutated proteins. The near-UV CD spectrum of wt sorcin is negative and characterized by two sharp bands at 262 and 268 nm attributed to phenylalanines, by a weaker band at 283 nm due to the tyrosyl fine structure (0−0 transition), and by a fairly intense, well-resolved peak at 292 nm due to tryptophan residues. The near-UV CD spectra (Figure 2B) of W105G display the peaks characteristic of the native protein, although the ellipticity is less negative. In contrast, the ellipticity of the W99G mutant in the 272−292 nm region is positive as in the case of Ca^{2+}-bound wt sorcin. A broad peak characterizes the fluorescence emission spectrum of apo-wt sorcin with a maximum at 338 nm, upon excitation at 280 nm. The intrinsic fluorescence of the two mutants is decreased with respect to that of wt sorcin, since most of the aromatic contribution at 280 nm is due to tryptophan residues (Figure 2C). The emission peak of the W99G mutant is blue shifted by 2 nm relative to that of wt sorcin, whereas the emission peak of W105G is red shifted by the same amount. Interestingly, in the 285−300 nm region, the spectra of the two variants are not additive, an indication that substitution of W99 or W105 influences the microenvironment of the other chromophores.

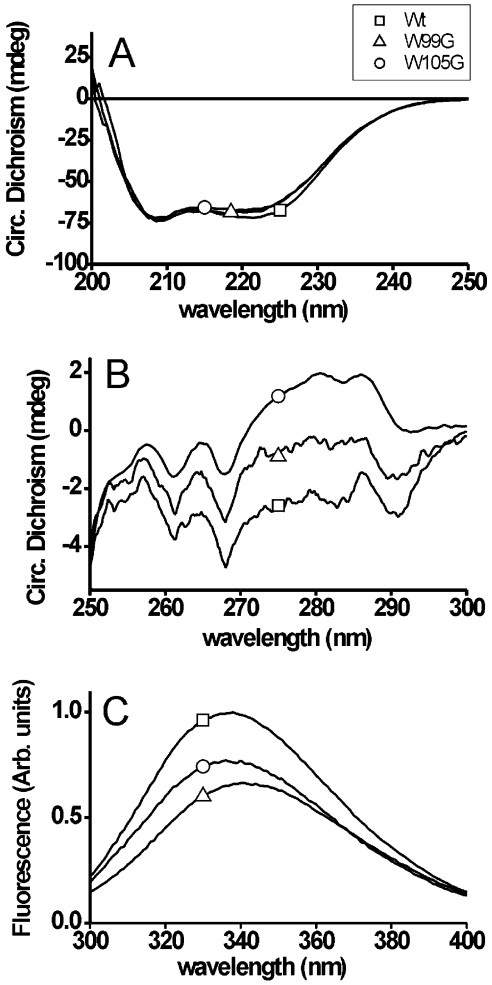

FIGURE 2: Spectroscopic characterization of wt sorcin and its W99G and W105G variants: wt (□), W99G (○), and W105G (△). (A) Far-UV CD spectra in 5 mM Tris-HCl (pH 7.5) at 20 °C with a protein concentration of 18 μM. (B) Near-UV CD spectra in 100 mM Tris-HCl (pH 7.5) and 2 mM EGTA at 20 °C with a protein concentration of 30 μM. (C) Fluorescence emission spectra in 100 mM Tris-HCl (pH 7.5) at 25 °C with a protein concentration of 4 μM, an excitation wavelength of 280 nm, and a slit width of 0.5 nm.

Sedimentation velocity experiments were used to assess the stoichiometry of Ca^{2+} binding. Solutions of 25 μM protein in Chelex-treated Tris-HCl buffer at pH 7.5 were titrated in the ultracentrifuge cell with up to 4 equiv of calcium/monomer. As for the wt protein (*16*), the $s_{20,w}$ value of W99G is always 3.2−3.3 S, although the absorbance at 280 nm decreases markedly when the level of calcium exceeds 2 equiv/monomer due to protein aggregation. W105G could not be analyzed since it precipitated out of solution even in the Chelex-treated buffer most likely due to the traces of metal leaking from the cell (Figure 3A).

The Ca^{2+} affinity of the sorcin variants was estimated by means of indirect fluorescence titration experiments in the presence of either Quin 2 or Fluo-3 as a Ca^{2+} chelator. The results obtained at pH 7.5 are presented in Figure 3B in terms of the degree of Quin 2 saturation as a function of total Ca^{2+} concentration. The data obtained with the mutants fall within the range of those measured in five different sets of experiments with wt sorcin. Accordingly, Ca^{2+} affinity is practically unaltered relative to that of wt sorcin and can be fitted with two Ca^{2+} binding constants in the micromolar

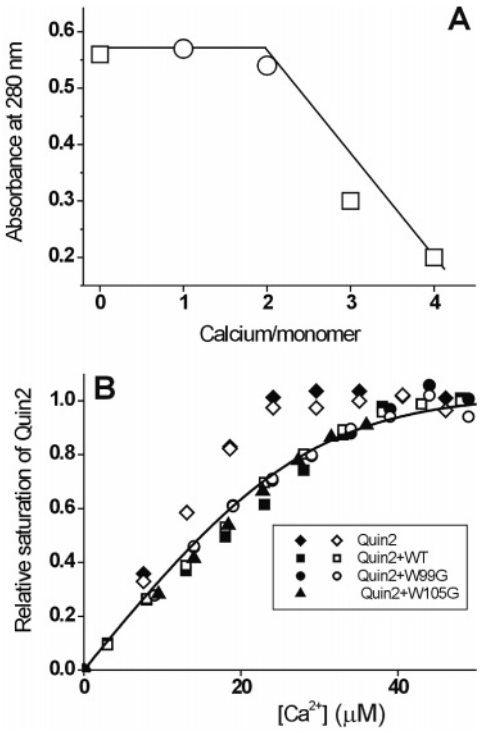

FIGURE 3: Calcium binding data. (A) Titration of W99G sorcin in the analytical ultracentrifuge. Different amounts of calcium were added just before the sedimentation velocity experiments to 15 μM protein in Chelex-treated 100 mM Tris-HCl buffer (pH 7.5). The absorbance in the plateau region is plotted as a function of the Ca^{2+}:monomer molar ratio. Different symbols refer to different experiments. (B) Fluorescence titration of wt sorcin and its W99G and W105G variants with Ca^{2+} in the presence of Quin 2. The relative saturation of Quin 2 is plotted as a function of total Ca^{2+} concentration. The wild type (□ and ■), W99G (○ and ●), and W105G (▲) sorcin at a concentration of 25 μM were titrated with Ca^{2+} in the presence of 25 μM Quin 2 in 100 mM Tris-HCl at pH 7.5 and 25 °C. Control titrations of Quin 2 alone with Ca^{2+} (◇ and ◆) are also shown.

range [$K_1 = (0.5 \pm 0.2) \times 10^{-6}$ M and $K_2 \sim 10^{-5}$ M] using a dissociation constant for the chelator of 60 nM (*25*). The K_1 value is better defined than K_2; the value of this latter binding constant is at the resolution limits of the technique under the conditions that were used. The Fluo-3 titration data are consistent with minor changes in Ca^{2+} affinity of the mutants with respect to wt sorcin (data not shown).

Interaction between the W99G and W105G Variants and Annexin VII. Overlay assay experiments were carried out first to establish whether W99G and W105G are able to recognize and interact with annexin VII. Previous data demonstrated that the sorcin−annexin VII interaction occurs via their respective N-terminal domains at micromolar Ca^{2+} concentrations (*15*, *31*). Western blot experiments indicate that binding of annexin VII to W99G is significant when the total Ca^{2+} concentration is 10 μM (Figure 4A), whereas comparable binding to W105G is observed when the cation concentration is increased to 75 μM (Figure 4B).

SPR was used to assess the effect of the mutations on the interaction between sorcin and annexin VII in a quantitative manner. At constant protein and Ca^{2+} concentrations, the steady-state signals (R_{eq}) obtained with wt sorcin and W99G are very similar and significantly higher than in the case of W105G (Figure 5A).

When the interaction is assessed as a function of Ca^{2+} concentration at a constant protein concentration, the R_{eq}

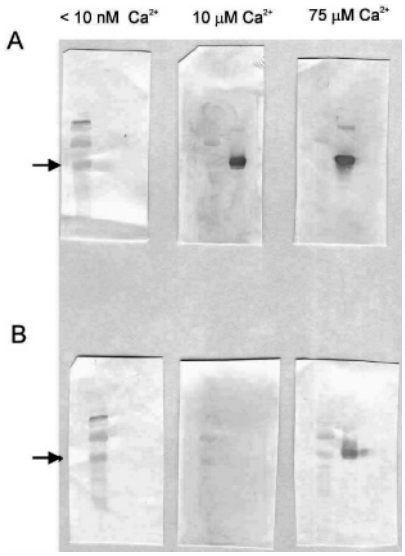

FIGURE 4: Interaction of the W99G and W105G sorcin variants with annexin VII. The variants were subjected to SDS−PAGE and transferred to PVDF membranes which were incubated with annexin VII in the presence of <10 nM, 10 μM, or 75 μM $CaCl_2$ (from left to right) and subsequently with anti-annexin monoclonal antibody. (A) W99G and (B) W105G: lane 1, molecular mass markers (46, 30, 21.5, 14.3, 6.5, and 3.4 kDa); and lane 2, sorcin variant. The arrows indicate the band corresponding to sorcin (M_r = 21.5 kDa). For buffer conditions, see Materials and Methods.

values show the expected increase with an increase in Ca^{2+} concentration **(**Figure 5B). The W99G variant behaves like wt sorcin at <40 μM Ca^{2+} but yields lower R_{eq} values at higher cation concentrations, while W105G gives rise to significantly lower sensorgrams with respect to wt sorcin at all Ca^{2+} concentrations that were investigated. At 50 μM Ca^{2+}, for example, the R_{eq} values are 385 for wt sorcin, 287 for W99G, and 79 for W105G. It follows that the affinity for the annexin N-terminus decreases in the following order: wt sorcin ≥ W99G > W105G. A further series of experiments was carried out as a function of protein concentration at a constant Ca^{2+} concentration of 20 μM (Figure 5C). This type of experiment enables one to assess the apparent dissociation constant, K_D, for each protein by Scatchard analysis of the ratio R_{eq}/C versus R_{eq} (*32*). The analysis yields apparent K_D values (at 20 μM Ca^{2+}) of 1.9 μM for wt sorcin, 2.0 μM for W99G, and 12.6 μM for W105G. In this calculation, the intercept on the abscissa was considered to be the same for the three proteins since the limited number of data and the low R_{eq} values at 20 μM Ca^{2+} pertaining to the W105G mutant do not warrant a precise R_{max} determination. If one assumes that the sorcin dimer contains a single effective annexin VII binding site as suggested by Brownawell and Creutz (*31*), the analysis yields K_D values of 0.95 μM for wt sorcin, 1.0 μM for W99G, and 6.3 μM for W105G.

Effect of the W99G and W105G Variants on the Activity of the Ryanodine Receptor. The protocol used to introduce recombinant protein into permeabilized myocytes is shown in Figure 6A. After being exposed to β-escin for 30 s, the myocyte was superfused with mock intracellular solution for 30 s before superfusing with 3 μM sorcin (or sorcin variants) for 2 min to ensure that the complete bath volume (200 μL) was exchanged with the protein-containing solution. Superfusion was stopped, and sparks were monitored in the

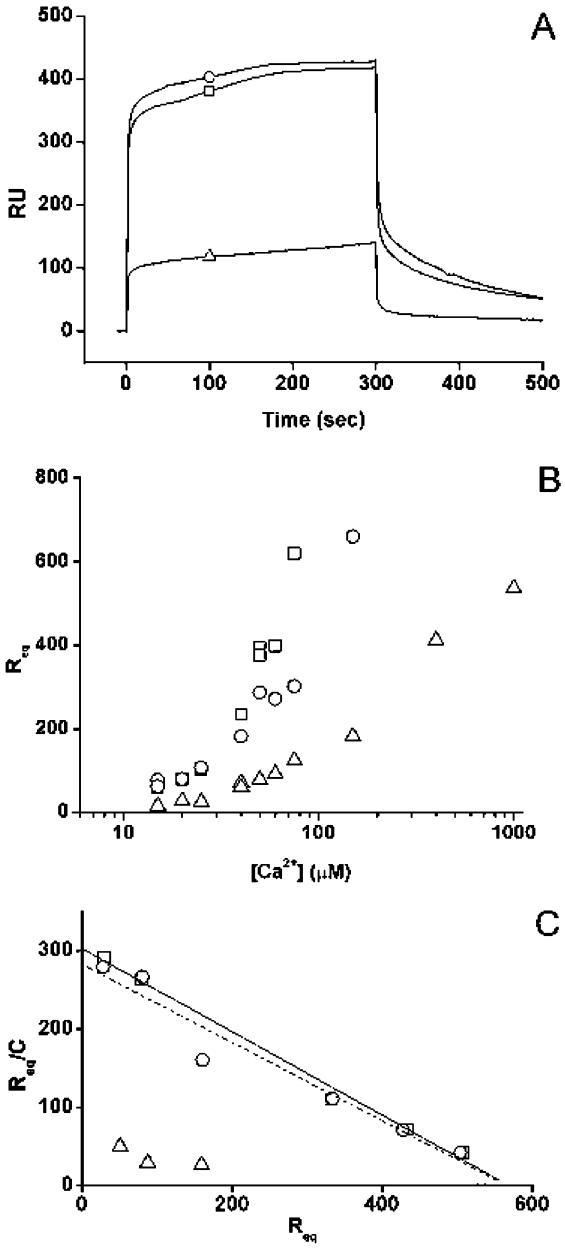

FIGURE 5: Binding of wt sorcin and its W99G and W105G variants to the immobilized N-terminal peptide of annexin VII at different Ca^{2+} concentrations: wt (□), W99G (○), and W105G (△). (A) Sensorgrams of 6 μM sorcin injected at time zero onto a chip containing the immobilized N-terminal annexin VII peptide. The increase in RU relative to baseline indicates complex formation; the plateau region represents the steady-state phase of the interaction, whereas the decrease in RU represents sorcin dissociation from the immobilized peptide after injection of buffer [10 mM HEPES, 0.15 M NaCl, 20 μM $CaCl_2$, and 0.005% surfactant P-20 (pH 7.4)]. The temperature was 25 °C. (B) The plateau signal at steady state (R_{eq}) is plotted as a function of total Ca^{2+} concentration. The sorcin concentration was 1 μM in 10 mM HEPES, 0.15 M NaCl, and 0.005% surfactant P-20 (pH 7.4). The temperature was 25 °C. (C) The plateau signal at steady state (R_{eq}) measured at different sorcin concentrations (C) is plotted as a function of R_{eq}/C. The buffer contained 10 mM HEPES, 0.15 M NaCl, 20 μM $CaCl_2$, and 0.005% surfactant P-20 (pH 7.4).

absence of flow for 10−12 min. Sample line-scan records are shown in Figure 6B showing the transient increases in intracellular Ca^{2+} concentration characteristic of Ca^{2+} sparks. Under control conditions, spark frequency progressively decreased by 20−25% over 10−12 min. As shown in Figure

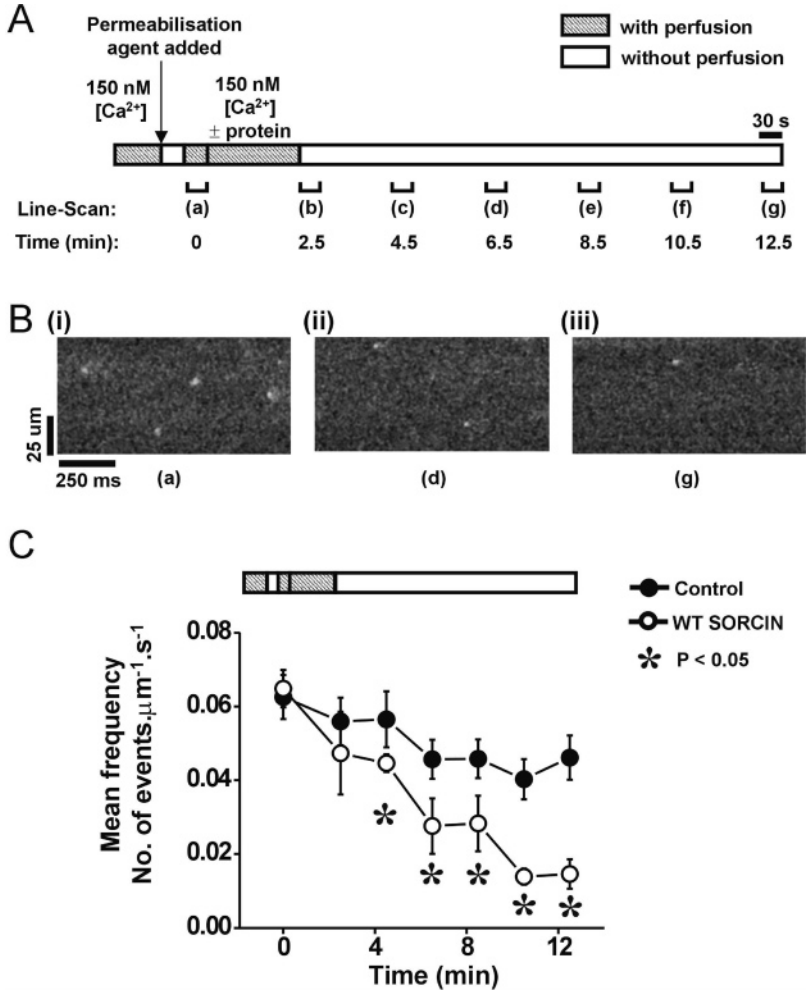

FIGURE 6: Ca^{2+} spark protocol. (A) Experimental protocol used to introduce recombinant protein into permeabilized myocytes. (B) Sample line scans 0 (a), 6 (d), and 12 min (g) after permeabilization. (C) Mean spark frequency at various times after permeabilization. Note the slow decline in spark frequency with time under control conditions. The inclusion of sorcin (3 μM) in the initial perfusing solution caused a profound decrease in frequency. Steady-state values were measured after incubation for 10−12 min with the recombinant protein.

6C, the inclusion of 3 μM sorcin in the perfusion solution caused a more marked decrease in spark frequency, reaching a steady state after 8−10 min. The difference caused by the presence of sorcin is likely to reflect the time course of entry of sorcin into the permeabilized cell. The effects of sorcin, W99G, W105G, E124A, and SCBD were studied by measuring the spark characteristics after incubation for 10 min with the protein. This activity was compared with that observed after incubation for the same time with a solution of the identical composition without the protein.

The inhibitory effect of sorcin on RyR2 activity manifests itself in the significant reduction of the mean values of Ca^{2+} spark frequency, spark width, spark peak, and spark duration compared to the control spark parameters (Figure 7A). The two tryptophan mutants have contrasting effects. W99G affects the Ca^{2+} spark parameters in a manner similar to that of the native protein (Figure 7B). In contrast, in the presence of W105G, the parameters of the Ca^{2+} sparks are close to those of the control cardiomyocytes (Figure 7C).

SCBD was used to test the possible effects of the sorcin N-terminal domain on formation of the RyR2−sorcin complex. SCBD decreases the mean values of the Ca^{2+} spark frequency and width in a manner similar to that of the full-length wt protein, while the mean duration and amplitude are not altered significantly with respect to the control cardiomyocytes (Figure 7D). The E124A mutant is unable to bind Ca^{2+} at physiological concentrations (*6*); perfusion with this mutant yields Ca^{2+} spark values very similar to those obtained under control conditions (Figure 7E).

DISCUSSION

These data provide experimental support to the model of sorcin activation that assigns a major role to the D helix which connects the two physiologically relevant sites, EF2 and EF3, and contains the only two tryptophan residues of the polypeptide chain, W99 and W105. The different location of the tryptophan residues along the D helix (W99 is ~4 Å from EF2 and W105 is ~7 Å from EF3) renders the W105G and W99G variants as selective probes of the Ca^{2+}-induced structural changes and of their functional effects. Their study therefore extends the information furnished by the mutants of the EF1, EF2, and EF3 hands studied by Mella et al. (*6*) which monitor the effect of abolishing binding of calcium to the respective EF-hand motifs.

The proposed model of sorcin activation explains an apparent paradox common to all PEF proteins: the large Ca^{2+}-dependent change in hydrophobicity would predict large conformational differences, yet only small Ca^{2+}-linked structural rearrangements limited to the EF1 region are

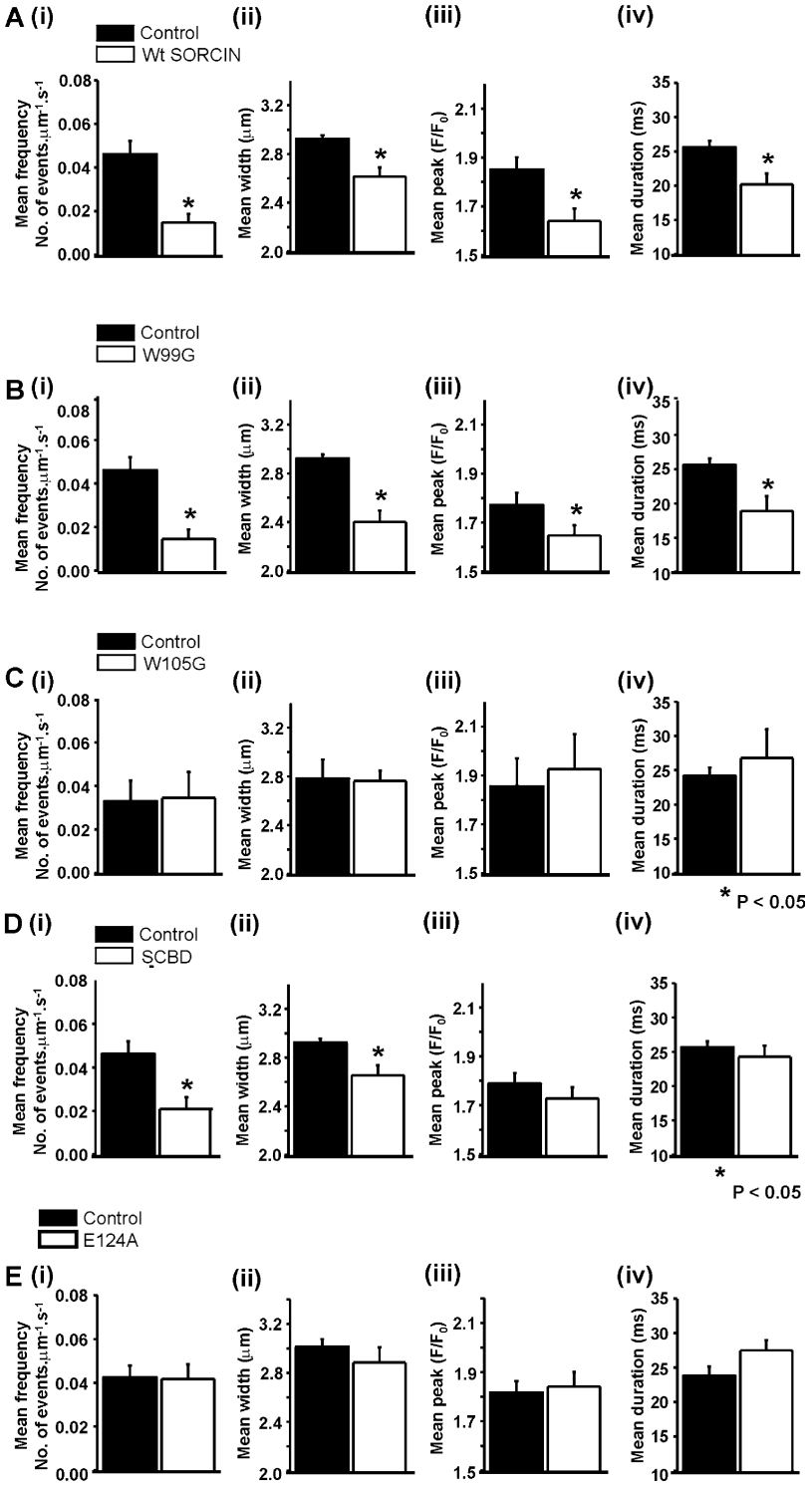

FIGURE 7: Effect of wt sorcin, of the W99G, W105G, and E124A variants, and of SCBD on Ca^{2+} spark properties. Mean values ± the standard error of the mean for (i) spark frequency, (ii) spark width (full width at half-maximum), (iii) peak F/F_o, and (iv) spark duration (full width at half-maximum). (A) Control group, $n = 4$ cells, 636 events; sorcin, $n = 4$ cells, 176 events. (B) Control group, $n = 5$ cells, 795 events; W99G group, $n = 5$ cells, 200 events. (C) Control group, $n = 4$ cells, 630 events; W105G group, $n = 4$ cells, 592 events. (D) Control group, $n = 4$ cells, 662 events; SCBD, $n = 5$ cells, 425 events. (E) Control group, $n = 7$ cells, 814 events; E124A group, $n = 7$ cells, 739 events. Asterisks indicate $P < 0.05$.

observed (*1*, *9*, *11*−*13*). On the basis of the crystal structure of SCBD, Ilari et al. (*7*) proposed that in Ca^{2+}-free sorcin the N- and C-terminal domains establish a large number of hydrophobic and hydrophilic interactions centered on the D helix. Both tryptophan residues are part of this interaction network which comprises the loop between EF1 and EF2 (Tyr67 aromatic ring) and reaches the Ca^{2+}-binding loop of EF3 where Asp113 in position X is hydrogen bonded to the Tyr67 OH group. Importantly, W99 and W105 together with other highly conserved D helix residues (Phe95, Leu98, and Phe109) give rise to a rather extended hydrophobic patch. However, whereas the W99 side chain lies on the outer surface of SCBD and establishes few van der Waals contacts with the very first residues of the domain, the W105 side

chain faces the SCBD core and establishes a large number of intradomain interactions with other residues of the D helix (Val101, Leu102, His108, and Phe109), of the EF loop (Met132 and Phe134), and of the long G helix (Tyr159, Ile160, Cys163, Val164, and Arg167).

In the SCBD model of the apoprotein which contains solely an 11-residue stretch of the N-terminus (*7*), W105 but not W99 is part of the SCBD region in contact with the N-terminal domain. The interdomain contact region comprises Val101, Leu102, Gly104, Trp105, and His108 in the D helix, Arg174 in the G helix, Met132, Gly133, Phe134, and Arg135 in the EF loop, and Gly182 in the GH loop and, therefore, many of the residues just mentioned. The possibility that W99 may be part of this contact region in the full-length protein where the N-terminal domain is 32 amino acids long cannot be excluded.

Ilari et al. (*7*) proposed that calcium binding loosens the network of interdomain interactions, rendering both domains available for target protein recognition. It follows that all the D helix residues which contact the N-terminal domain in the apoprotein may participate in the interaction with molecular targets in Ca^{2+}-bound sorcin. In principle, such interaction can be very diversified as it will depend on the specific position of a given residue in the contact region. On this basis, removal of W99, which is located near EF2 on the outer surface of SCBD and is only marginally involved in interdomain interactions, is expected to have functional ramifications very different from those of removal of W105 which faces the SCBD core near the highest-Ca^{2+} affinity EF3 site.

Ca^{2+} Binding and Association with Annexin VII. The site-specific mutations that are introduced do not alter the overall structure of wt sorcin significantly as shown by the sedimentation velocity data and far-UV CD spectra (Figure 2A), although local structural perturbations are apparent in the fluorescence emission (Figure 2C) and near-UV CD spectra (Figure 2B). However, in the absence of structural data in the crystalline state, these spectroscopic methods do not permit extrapolation to specific structural and functional features (*33*). For example, the near-UV CD spectrum of W99G resembles that of Ca^{2+}-bound wt sorcin and that of W105G resembles that of the Ca^{2+}-free form, yet both mutants require Ca^{2+} for interaction with annexin VII (Figure 5B). The absence of the negative tryptophan peak at 292 nm in the CD spectrum of W99G sorcin and its reduction in the W105G variant, just like the differences in the fine structure of the whole spectrum, point to the occurrence of specific local perturbations in the environment of aromatic residues attendant the mutations introduced. In particular, in the W99G variant, Trp105 could be more exposed to solvent than in apo-wt sorcin as is the case of the Ca^{2+}-ligated wt protein. A similar albeit smaller decrease in the tryptophan band at 292 nm was observed in the E124A variant, where the hydrogen bonding interactions established by Asp113 and Glu124 of the EF3 Ca^{2+} binding loop are lost (*6*). This similarity is indicative of similar structural rearrangements and likely is functionally relevant.

The measurements of the Ca^{2+} binding parameters are confined to a limited set of experimental conditions given the strong tendency of the Ca^{2+}-bound form of wt sorcin and in particular of W105G to aggregate and/or precipitate in the absence of protein targets. As a consequence, determination of the weaker Ca^{2+} binding constant will be particularly affected. Within these limitations, neither mutation appears to affect Ca^{2+} binding significantly (Figure 3). Thus, calcium titrations carried out in the ultracentrifugation show that the W99G variant binds two Ca^{2+} ions per monomer with an affinity similar to that of wt sorcin (*16*). The titration data obtained for the two variants in the presence of Quin 2 as the reporter dye likewise do not provide evidence for significant changes in Ca^{2+} affinity with respect to wt sorcin. The use of Fluo-3 did not improve accuracy (data not shown).

The Ca^{2+} sensitivity of annexin VII binding is unaltered by the W99G mutation but is decreased significantly ($\approx$7 times) by the W105G mutation. In the framework of a linkage scheme, any change in the Ca^{2+} sensitivity of annexin VII binding can be attributed to a change in either calcium or target binding or both steps. In the W105G variant, since Ca^{2+} affinity is essentially unchanged relative to that of wt sorcin (Figure 3B), it is primarily the interaction with the target that is affected by the mutation. The factors that come into play are (i) impairment of information transfer via the D helix and (ii) alterations in the recognition surfaces required for sorcin N-terminal domain interaction. The latter option is unlikely since the local structural changes induced by Ca^{2+} binding and propagated via the D helix will affect mainly the relative orientation of the C- and N-terminal domains (*7*) and will only weakly alter the structure of the N-terminal domain itself.

Ca^{2+} Spark Activity. The plot of Ca^{2+} spark frequency shown in Figure 6 indicates a small but significant reduction in spark frequency over 10−12 min. The cause of these changes is unknown but may reflect the balance of several factors, including (i) a change in the Ca^{2+} content of the SR immediately after permeabilization and (ii) minor changes in concentration of low-molecular weight modulators of RyR2 activity, e.g., ATP, Mg^{2+}, H^+. The reduced frequency, amplitude, duration, and width of the Ca^{2+} spark by wt sorcin (Figure 7A) are consistent with previous reports on heart cells (*18*, *19*, *34*). Measurements on isolated RyR2 channels indicate that sorcin reduces the open time of the channel but does not affect single-channel conductance (*18*). A reduced open time would reduce the duration of the Ca^{2+} spark and therefore the amplitude and width. The effect on Ca^{2+} spark frequency may be linked to the reduced open probability of the channel at a set intracellular Ca^{2+} concentration (*18*). As with the previous work, the additional Ca^{2+} buffering attributable to sorcin is unlikely to be a complicating factor. The background Ca^{2+} buffers both in the perfusing solution and intrinsic to the permeabilized cell are present at >10 times the concentration of exogenous sorcin.

The effects of sorcin on Ca^{2+} sparks are evident at 155−165 nM Ca^{2+}, where the EF3 site is only 15% saturated. Considering local versus bulk concentration during a Ca^{2+} spark easily accounts for this apparent contradiction (*34*). Thus, within limited regions of the cytosol close to the Ca^{2+} entry and release sites, the cation concentration may rise to >10 μM and hence be sufficient to trigger the sorcin conformational changes.

The tryptophan variants have strikingly different effects on Ca^{2+} spark activity. The effects of W99G are similar in all respects to those of the wt protein and suggest that despite

the local structural changes indicated above, Ca^{2+} binding, information transfer through the D helix, and RyR2 recognition occur normally. In contrast to W99G, the W105G mutant has no significant effects on any of the Ca^{2+} spark parameters, indicating that this mutation dramatically alters either information transfer or the interaction surface with RyR2, since it does not impair Ca^{2+} binding. The ability of W105G to bind annexin VII, albeit with a lower Ca^{2+} sensitivity (Figure 5C), indicates that information about the Ca^{2+} binding event does reach the N-terminal domain and suggests that the mutation of this tryptophan affects mainly the RyR2 recognition surface. One additional explanation for differential effects of the W105G variant compared to the wt sorcin or to the W99G mutant is that the W105G variant may be phosphorylated by protein kinase A more readily than the other two proteins (*18*). The SCBD fragment, which cannot bind annexin VII, is able to interact successfully with RyR from skeletal muscle based on previous biochemical data (*16*) and on the significant reduction in Ca^{2+} spark frequency and width (Figure 7D). Interestingly, SCBD appears not to significantly affect Ca^{2+} spark peak and duration. Over the complete range of Ca^{2+} spark parameters, there is the overall impression of a weaker effect of SCBD on RyR2 activity. This may reflect a minor involvement of the N-terminal domain in the association process or simply the fact that the interaction surface is altered slightly by removal of the N-terminal domain. The E124A mutation, which disrupts coordination of Ca^{2+} at the EF3 site, ablates the ability of the variant both to bind annexin VII (*6*) and to reduce RyR2 activity (Figure 7E). This confirms that binding of Ca^{2+} to sorcin (EF3 site) is an absolute requirement for interaction with target proteins (*6*).

In conclusion, these data provide experimental support to the proposal that the interaction network around the D helix is central to the Ca^{2+}-induced activation mechanism of sorcin. The D helix acts as an amplifier of the conformational changes that take place at the EF3 loop upon Ca^{2+} binding by triggering a larger overall change that enables sorcin to interact with its target proteins. In view of the D helix conservation, it is likely that the same activation mechanism applies to all PEF proteins. Additionally, this study brings out the crucial role of Trp105 and not Trp99 in allowing sorcin to interact with RyR2. Extension of this approach to other protein targets, e.g., α_1 subunit of the L-type Ca^{2+} channel (*35*) and the cardiac Na^+/Ca^{2+} exchanger, will clarify whether this approach can be generalized to mapping the topology of the interaction of sorcin with its targets.

ACKNOWLEDGMENT

We thank Dr. Bruno Catacchio for carrying out the analytical ultracentrifuge experiments. The technical assistance of Aileen Rankin and Anne Ward is gratefully acknowledged.

REFERENCES

1. Blanchard, H., Grochulski, P., Li, Y., Arthur, S. C., Davies, P. L., Elce, J. S., and Cygler, M. (1997) Structure of a calpain Ca^{2+}-binding domain reveals a novel EF-hand and Ca^{2+}-induced conformational changes, *Nat. Struct. Biol. 4*, 532−538.
2. Lin, G. D., Chattopadhyay, D., Maki, M., Wang, K. K., Crason, M., Jin, L., Yuen, P. W., Takano, E., Hatanaka, M., DeLucas, L. J., and Narayana, S. V. (1997) Crystal structure of calcium bound domain VI of calpain at 1.9 Å resolution and its role in enzyme assembly, regulation, and inhibitor binding, *Nat. Struct. Biol. 4*, 539−547.
3. Lollike, K., Johnsen, A. H., Durussel, I., Borregaard, N., and Cox, A. (2001) Biochemical characterization of the penta-EF-hand protein grancalcin and identification of L-plastin as a binding partner, *J. Biol. Chem. 276*, 17762−17769.
4. Lo, K. W.-H., Zhang, Q., Li, M., and Zhang, M. (1999) Apoptosis-linked gene product ALG-2 is a new member of the calpain small subunit subfamily of Ca^{2+}-binding proteins, *Biochemistry 38*, 7498−7508.
5. Kitaura, Y., Matsumoto, S., Satoh, H., Hitomi, K., and Maki, M. (2001) Peflin and ALG-2, members of the penta-EF-hand protein family, form a heterodimer that dissociates in a Ca^{2+}-dependent manner, *J. Biol. Chem. 276*, 14053−14058.
6. Mella, M., Colotti, G., Zamparelli, C., Verzili, D., Ilari, A., and Chiancone, E. (2003) Information transfer in the penta-EF-hand protein sorcin does not operate via the canonical structural/functional pairing. A study with site-specific mutants, *J. Biol. Chem. 278*, 24921−24928.
7. Ilari, A., Johnson, K. A., Nastopoulos, V., Verzili, D., Zamparelli, C., Colotti, G., Tsernoglou, D., and Chiancone, E. (2002) The crystal structure of the sorcin calcium binding domain provides a model of Ca^{2+}-dependent processes in the full-length protein, *J. Mol. Biol. 317*, 447−458.
8. Xie, X., Dwyer, M. D., Swenson, L., Parker, M. H., and Botfield, M. C. (2001) Crystal structure of calcium-free human sorcin: A member of the penta-EF-hand protein family, *Protein Sci. 10*, 2419−2425.
9. Jia, J., Han, Q., Borregaard, N., Lollike, K., and Cygler, M. (2000) Crystal structure of human grancalcin, a member of the penta-EF-hand protein family, *J. Mol. Biol. 300*, 1271−1281.
10. Jia, J., Tarabykina, S., Hansen, C., Berchtold, M., and Cygler, M. (2001) Structure of apoptosis-linked protein ALG-2: Insights into Ca^{2+}-induced changes in penta-EF-hands proteins, *Structure 4*, 267−275.
11. Jia, J., Borregaard, N., Lollike, K., and Cygler, M. (2001) Structure of Ca^{2+}-loaded human grancalcin, *Acta Crystallogr. D57*, 1843−1849.
12. Strobl, S., Fernandez-Catalan, C., Braun, M., Huber, R., Masumoto, H., Nakagawa, K., Irie, A., Sorimachi, H., Bourenkow, G., Bartunik, H., Suzuki, K., and Bode, W. (2000) The crystal structure of calcium-free human m-calpain suggests an electrostatic switch mechanism for activation by calcium, *Proc. Natl. Acad. Sci. U.S.A. 97*, 588−592.
13. Hosfield, C. M., Elce, J. S., Davies, L., and Jia, Z. (1999) Crystal structure of calpain reveals the structural basis for Ca^{2+}-dependent protease activity and a novel mode of enzyme activation, *EMBO J. 18*, 6880−6889.
14. Meyers, M. B., Pickel, v. M., Sheu, S.-S., Sharma, V. K., Scotto, K. W., and Fishman, G. I. (1995) Association of sorcin with the cardiac ryanodine receptor, *J. Biol. Chem. 270*, 26411−26418.
15. Verzili, D., Zamparelli, C., Mattei, B., Noegel, A. A., and Chiancone, E. (2000) The sorcin-annexin VII calcium-dependent interaction requires the sorcin N-terminal domain, *FEBS Lett. 471*, 197−200.
16. Zamparelli, C., Ilari, A., Verzili, D., Giangiacomo, L., Colotti, G., Pascarella, S., and Chiancone, E. (2000) Structure−function relationships in sorcin, a member of the penta EF-hand family. Interaction of sorcin fragments with the ryanodine receptor and an *Escherichia coli* model system, *Biochemistry 39*, 658−666.
17. Cheng, H., Lederer, W. J., and Camnel, M. B. (1993) Calcium sparks: Elementary events underlying excitation-contraction coupling in heart muscle, *Science 262*, 740−744.
18. Lokuta, C. J., Meyers, M. B., Sander, P. R., Fishman, G. I., and Valdivia, H. H. (1997) Modulation of cardiac ryanodine receptors by sorcin, *J. Biol. Chem. 272*, 25333−25338.
19. Seidler, T., Miller, S. L. W., Loughrey, C. M., Kania, A., Burow, A., Kettlewell, S., Teucher, N., Wagner, S., Kogler, H., Meyers, M. B., Hasenfuss, G., and Smith, G. L. (2003) Effects of adenovirus-mediated sorcin overexpression on excitation-contraction coupling in isolated rabbit cardiomyocytes, *Circ. Res. 93*, 132−139.
20. Maki, M., Kitaura, Y., Satoh, H., Ohkouchi, S., and Shibata, H. (2002) Structures, functions and molecular evolution of the penta-EF-hand Ca^{2+}-binding proteins, *Biochim. Biophys. Acta 1600*, 51−60.
21. Higuchi, R., Krummel, B., and Saiki, R. K. (1988) A general method of in vitro preparation and specific mutagenesis of DNA

fragments: Study of protein and DNA interactions, *Nucleic Acid Res. 16*, 7351−7367.
22. Meyers, M. B., Zamparelli, C., Verzili, D., Dicker, A. P., Blanck, T. J. J., and Chiancone, E. (1995) Calcium-dependent translocation of sorcin to membranes: Functional relevance in contractile tissue, *FEBS Lett. 357*, 230−234.
23. Edelhoch, H. (1967) Spectroscopic determination of tryptophan and tyrosine in proteins, *Biochemistry 6*, 1948−1954.
24. Chou, P. Y., and Fasman, G. D. (1974) Prediction of protein conformation, *Biochemistry 13*, 222−224.
25. Tsien, R., and Pozzan, T. (1989) Measurement of cytosolic free Ca^{2+} with Quin 2, *Methods Enzymol. 172*, 230−262.
26. Zamparelli, C., Ilari, A., Verzili, D., Vecchini, P., and Chiancone, E. (1997) Calcium- and pH-linked oligomerization of sorcin causing translocation from cytosol to membranes, *FEBS Lett. 409*, 1−6.
27. André, I., and Linse, S. (2002) Measurement of Ca^{2+}-binding constants of proteins and presentation of the CaLigator software, *Anal. Biochem. 305*, 195−205.
28. Laemmli, U. K. (1970) Cleavage of structural proteins during the assembly of the head of the bacteriophage T4, *Nature 227*, 680−685.
29. Bjellqvist, B., Hughes, G. J., Pasquali, Ch., Paquet, N., Ravier, F., Sanchez, J. C., Frutiger, S., and Hochstrasser, D. F. (1993) The focusing positions of polypeptides in immobilized pH gradients can be predicted from their amino acid sequences, *Electrophoresis 14*, 1023−1031.
30. *BIAtechnology Handbook*, version AB (1994) pp 4−5, Biacore AB, Uppsala, Sweden.
31. Brownawell, A. M., and Creutz, C. E. (1997) Calcium-dependent binding of sorcin to the N-terminal domain of synexin (annexin VII), *J. Biol. Chem. 272*, 22182−22190.
32. Schuck, P. (1997) Use of surface plasmon resonance to probe the equilibrium and dynamic aspects of interactions between biological macromolecules, *Annu. Rev. Biophys. Biomol. Struct. 26*, 541−566.
33. Strickland, E. H. (1974) Aromatic contributions to circular dichroism spectra of proteins, *CRC Crit. Rev. Biochem.*, 113−175.
34. Farrell, E. F., Antaramian, A., Rueda, A., Gomez, A. M., and Valdivia, H. H. (2003) Sorcin inhibits calcium release and modulates excitation-contraction coupling in the heart, *J. Biol. Chem. 278*, 34660−34666.
35. Meyers, M. B., Puri, T. S., Chien, A. J., Gao, T., Hsu, P.-H., Hosey, M. M., and Fishman, G. I. (1998) Sorcin associates with the pore-forming subunit of voltage-dependent L-type Ca^{2+} channels, *J. Biol. Chem. 273*, 18930−18935.
36. DeLano, W. L. (2002) *The PyMOL User's Manual*, DeLano Scientific, San Carlos, CA.

BI060416A